Neuro-Oncology

21(4), 517–526, 2019 | doi:10.1093/neuonc/noy160 | Advance Access date 1 October 2018

Combined iron oxide nanoparticle ferumoxytol and gadolinium contrast enhanced MRI define glioblastoma pseudoprogression

Ramon F. Barajas Jr,* Bronwyn E. Hamilton,* Daniel Schwartz, Heather L. McConnell, David R. Pettersson, Andrea Horvath, Laszlo Szidonya, Csanad G. Varallyay, Jenny Firkins, Jerry J. Jaboin, Charlotte D. Kubicky, Ahmed M. Raslan, Aclan Dogan, Justin S. Cetas, Jeremy Ciporen, Seunggu J. Han, Prakash Ambady, Leslie L. Muldoon, Randy Woltjer, William D. Rooney, and Edward A. Neuwelt

Department of Radiology (R.F.B., B.E.H., D.R.P., C.G.V.), Advanced Imaging Research Center (R.F.B., D.S., A.H., W.D.R.), Department of Neurology (D.S., H.L.M., L.S., C.G.V., J.F., P.A., L.L.M., E.A.N.), Radiation Medicine (J.J.J., C.D.K.), Neurological Surgery (A.M.R., A.D., J.S.C., J.C., S.J.H, E.A.N.), Portland Veterans Affairs Medical Center, Portland, Oregon (E.A.N.); Department of Pathology, Oregon Health and Science University, Portland, Oregon (R.W.)

Corresponding Author: Edward A. Neuwelt MD, Blood-Brain Barrier Program, Oregon Health and Science University, Portland, OR 97239 (neuwelte@ohsu.edu).

*These authors contributed equally to this manuscript.

Abstract

Background. Noninvasively differentiating therapy-induced pseudoprogression from recurrent disease in patients with glioblastoma is prospectively difficult due to the current lack of a biologically specific imaging metric. Ferumoxytol iron oxide nanoparticle MRI contrast characterizes innate immunity mediated neuroinflammation; therefore, we hypothesized that combined ferumoxytol and gadolinium enhanced MRI could serve as a biomarker of glioblastoma pseudoprogression.

Methods. In this institutional review board-approved, retrospective study, we analyzed ferumoxytol and gadolinium contrast enhanced T1-weighted 3T MRI in 45 patients with glioblastoma over multiple clinical timepoints. Isocitrate dehydrogenase 1 (IDH-1) mutational status was characterized by exome sequencing. Sum of products diameter measurements were calculated according to Response Assessment in Neuro-Oncology criteria from both gadolinium and ferumoxytol enhanced sequences. Enhancement mismatch was calculated as the natural log of the ferumoxytol to gadolinium sum of products diameter ratio. Analysis of variance and Student's *t*-test assessed differences in mismatch ratios. *P*-value <0.05 indicated statistical significance.

Results. With the development of pseudoprogression we observed a significantly elevated mismatch ratio compared with disease recurrence ($P < 0.01$) within IDH-1 wild type patients. Patients with IDH-1 mutation demonstrated significantly reduced mismatch ratio with the development of pseudoprogression compared with disease recurrence ($P < 0.01$). Receiver operator curve analysis demonstrated 100% sensitivity and specificity for the use of mismatch ratios as a diagnostic biomarker of pseudoprogression.

Conclusion. Our study suggests that ferumoxytol to gadolinium contrast mismatch ratios are an MRI biomarker for the diagnosis of pseudoprogression in patients with glioblastoma. This may be due to the unique characterization of therapy-induced neuroinflammation.

Key Point

Our study suggests that ferumoxytol to gadolinium contrast mismatch ratios are an MRI biomarker for the diagnosis of pseudo-progression in patients with glioblastoma. This may be due to the unique characterization of therapy-induced neuroinflammation.

Importance of the study

The findings of this retrospective study suggest that ferumoxytol and gadolinium contrast enhanced MRI mismatch ratio improves upon the diagnostic capability for differentiating pseudoprogression from disease recurrence in patients with IDH-1 wild type and mutated glioblastoma following temozolomide-based chemoradiotherapy. Image guided tissue sampling suggests that dual contrast mismatch may localize activated innate immunity within the tumor microenvironment. Future studies will determine if dual contrast MRI provides a biologically specific measure for the assessment of glioblastoma response to standard of care therapy.

The first-line treatment for patients with newly diagnosed glioblastoma is maximal safe resection followed by temozolomide-based chemoradiotherapy (CRT).[1–7] In some patients with glioblastoma, CRT leads to transiently increased volumes of contrast enhancement within the radiation field (pseudoprogression) on serial gadolinium enhanced T1-weighted MRI examinations (Gd-MRI).[8–13] The development of pseudoprogression is clinically relevant, as unlike patients with true disease recurrence, these patients will resolve their enhancing lesion without intervention and experience longer survival.[14] The etiology of pseudoprogression is hypothesized to be CRT mediated neuroinflammation.[8–11] At the cellular level, methylation of the DNA repair enzyme O^6-methylguanine-DNA methyltransferase (MGMT) promoter and mutated forms of the isocitrate dehydrogenase 1 (IDH-1) protein may contribute to development of pseudoprogression, albeit through different mechanisms.[15–27]

There is currently no clinically validated, biologically specific imaging biomarker that can differentiate neuroinflammation-mediated pseudoprogression from disease recurrence.[28] Serial Gd-MRI is clinically utilized to assess therapeutic response. The Response Assessment in Neuro-Oncology (RANO) Working Group has suggested the use of sum of products diameter (SPD) measurements as a biomarker of therapy response.[13] However, gadolinium SPD cannot reliably differentiate between the 2 phenomena, as apparent recurrent disease (a 25% increase in the Gd-MRI SPD) has been shown to represent pseudoprogression in up to 64% of cases.[8–13] This nonspecificity is due to the leakage of gadolinium through the disrupted neurovascular unit and subsequent enhancement within both the treated tumor interstia and inflamed neuropial compartments.[28–32] This makes prospectively diagnosing pseudoprogression nearly impossible with T1-weighted Gd-MRI. Previous investigators have developed perfusion Gd-MRI (cerebral blood volume [CBV]) and amino acid PET techniques that improve upon the limitations of T1-weighted Gd-MRI and provide quantifiable diagnostic measures of pseudoprogression. Clinical trials assessing diagnostic capabilities and clinical utility are currently underway.[33]

Preclinical models of brain tumor associated neuroinflammation have shown great promise for localizing sites of activated innate immunity with ferumoxytol contrast enhanced MRI (Fe-MRI).[34] Ferumoxytol is an ultrasmall superparamagnetic iron oxide nanoparticle that is FDA approved for iron replacement therapy and can be used off-label as an MRI contrast agent.[35] Like gadolinium, ferumoxytol shortens proton relaxation times, causing measurable signal changes on T1-weighted MRI 24 hours following intravenous administration (delayed phase).[34–37] Ferumoxytol is phagocytosed by tumor-associated macrophages (TAMs), which are known to infiltrate the tumor microenvironment during neuroinflammation.[34] Therefore, we hypothesized that the addition of 24-hour delayed phase Fe-MRI to standard of care gadolinium sequences could serve as a biomarker of neuroinflammation-mediated pseudoprogression.

The aim of this retrospective study was to determine whether the mismatch of the Gd-MRI T1 enhancement, a proxy for blood–brain barrier disruption, and the Fe-MRI T1 enhancement, a proxy for the concentration of inflammatory infiltrate, can better determine glioblastoma treatment outcome. We show that combined Fe- and Gd-MRI can uniquely identify the development of neuroinflammation-mediated pseudoprogression. Unlike RANO-recommended SPD measurements alone, the mismatch ratio of ferumoxytol to gadolinium enhancement SPD is diagnostic of pseudoprogression in both IDH-1 mutated and wild type glioblastoma as well as in nonmethylated MGMT promoter tumors.

Materials and Methods

Patient Population

This retrospective, institutional review board approved study included the following inclusion criteria: (i) histologically confirmed diagnosis of glioblastoma (World Health Organization classification grade IV), (ii) documentation of IDH-1 mutational status (R132H), (iii) a Karnofsky performance score >50, (iv) Gd-MRI within 72 hours prior to Fe-MRI at least once during the course of therapy, and (v) at least one instance of 24 hours delayed T1-weighted Fe-MRI. Using these inclusion criteria, we identified 45 patients who were studied at our institution between January 2012 and January 2017 (34 males, 12 females; mean age 56 ± 14 y). All patient Gd- and Fe-MRI examinations were classified as having occurred at 1 of 5 clinically relevant timepoints: preoperative = MRI examination occurred prior to surgical resection; postoperative = MRI examination occurred after maximally safe surgical resection but prior to radiation therapy; postradiation = MRI examination occurred within 3 months following the last date of radiation therapy; follow-up = MRI examination occurred more than 3 months following last date of radiation therapy but before development of progressive gadolinium contrast enhancement concerning for disease progression per RANO criteria; and

disease progression according to RANO criteria. At time of disease progression patients were either diagnosed as disease recurrence = progression of disease according to tissue histological analysis or patient clinical status and RANO criteria or pseudoprogression = according to RANO criteria established by serial follow-up Gd-MRI.

The retrospective nature precluded longitudinal Fe-enhanced MRI through the course of therapy. As such, all imaging data were taken to be cross-sectional. Of the 45 patients studied (39 IDH wild type, 6 with IDH mutation), 42 patients had Gd- and Fe-MRI performed at the time of disease progression (disease recurrence or pseudoprogression) in addition to earlier timepoints. The 3 patients without Gd- and Fe-MRI at time of disease progression all belonged to the IDH wild type cohort. Two of these patients had Gd- and Fe-MRI performed sequentially only at the preoperative, postoperative, postradiation, and follow-up timepoints, and 1 of these patients had Gd- and Fe-MRI only at the postoperative timepoint. None of the patients who met the inclusion criteria were excluded from analysis. MGMT status was noted when available. All patients underwent standard of care maximal safe resection followed by CRT.[2,3] Adjuvant radiotherapy consisted of 60 Gy in 2-Gy fractions or 40 Gy in 2.67-Gy fractions delivered using 3D conformal technique, intensity modulated radiotherapy, or volumetric modulated arc therapy concurrent with adjuvant temozolomide.

Review of the medical record established the diagnosis of disease recurrence or pseudoprogression for all 42 patients with Gd- and Fe-MRI at the time of disease progression. Seven patients underwent standard of care re-resection at the time of disease progression to establish disease status via histological analysis. All 7 of these patients (all IDH wild type) were diagnosed with disease recurrence. The remaining 35 patients had the diagnosis of either pseudoprogression or disease recurrence established by the integration of patient clinical course and serial Gd-MRI.

MRI Protocol

All patients underwent 3T MRI examinations using one of 2 imaging protocols (Fig. 1). Imaging protocol #1 (21 patients) entailed MRI on 3 consecutive days. In imaging protocol #2 (24 patients), MRI was performed on 2 consecutive days. Spin-echo T1-weighted images (repetition time/echo time = 900 ms/10 ms; field of view = 180 × 240 mm; imaging matrix = 192 × 256; axial slices = 44 contiguous 1 mm^2 thick; in-plane resolution = 0.9375 × 0.9375 mm^2) were acquired pre- and post-gadoteridol gadolinium chelate administration (0.1 mmol/kg; ProHance, Bracco Diagnostic) and ferumoxytol (Feraheme, provided free of charge by AMAG Pharmaceuticals), which was given over 20 min at a dose of up to 510 mg diluted to a final volume of 34 mL in normal saline. T1-weighted images were acquired 24 hours after i.v. ferumoxytol administration in order to visualize delayed enhancement. All imaging timepoints were completed on the same MRI instrument for each participant.

MRI Analysis

All data were acquired (J.F. and C.V., with more than 10 years experience), processed (R.B. and D.S., with more than 10 years experience), and analyzed (R.B., B.H., and D.P., with more than 10 years experience) using a standardized protocol for calculating enhancement measurements. Three attending radiologists with an American Board of Radiology certificate-added qualification in neuroradiology (R.B., B.H., and D.P.) were blinded to all clinical information, including treatment status and molecular profile status at the time of image analysis. R.B. first measured SPD on both the gadolinium and the ferumoxytol enhanced T1-weighted MRI. B.H. and D.P. subsequently and independently reviewed measurements made by R.B. and either agreed with the measurement or disagreed, in which case they made their own independent measurement. All measurements were made according to RANO criteria using commercially available software (IMPAX 6.5.5; Agfa Corporation) (Fig. 2A). Intraclass correlation coefficients (ICCs) (2,1) were calculated separately for gadolinium and ferumoxytol enhanced SPD measurements across the 3 raters.

Statistical Analysis

Contrast enhancement mismatch was calculated as the natural log (Ln) of the ratio of the 24-hour delayed phase

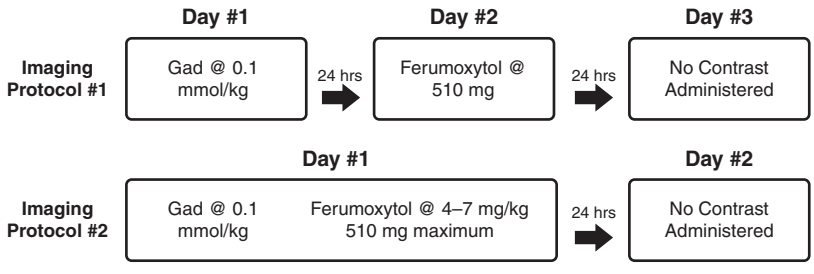

Fig. 1 Diagram of MRI protocols. Protocol #1 consisted of 3 days total MRI; day 1 included gadolinium enhanced imaging, day 2 consisted of vascular phase ferumoxytol enhanced MRI, and day 3 consisted of 24-hour delayed phase ferumoxytol MRI. Protocol #2 consisted of 2 days total MRI; day 1 consisted of gadolinium enhanced MRI followed by intravenous ferumoxytol contrast administration. Day 2 consisted of 24-hour delayed phase ferumoxytol enhanced MRI. No intravenous contrast was provided on the final day of MRI for either protocol.

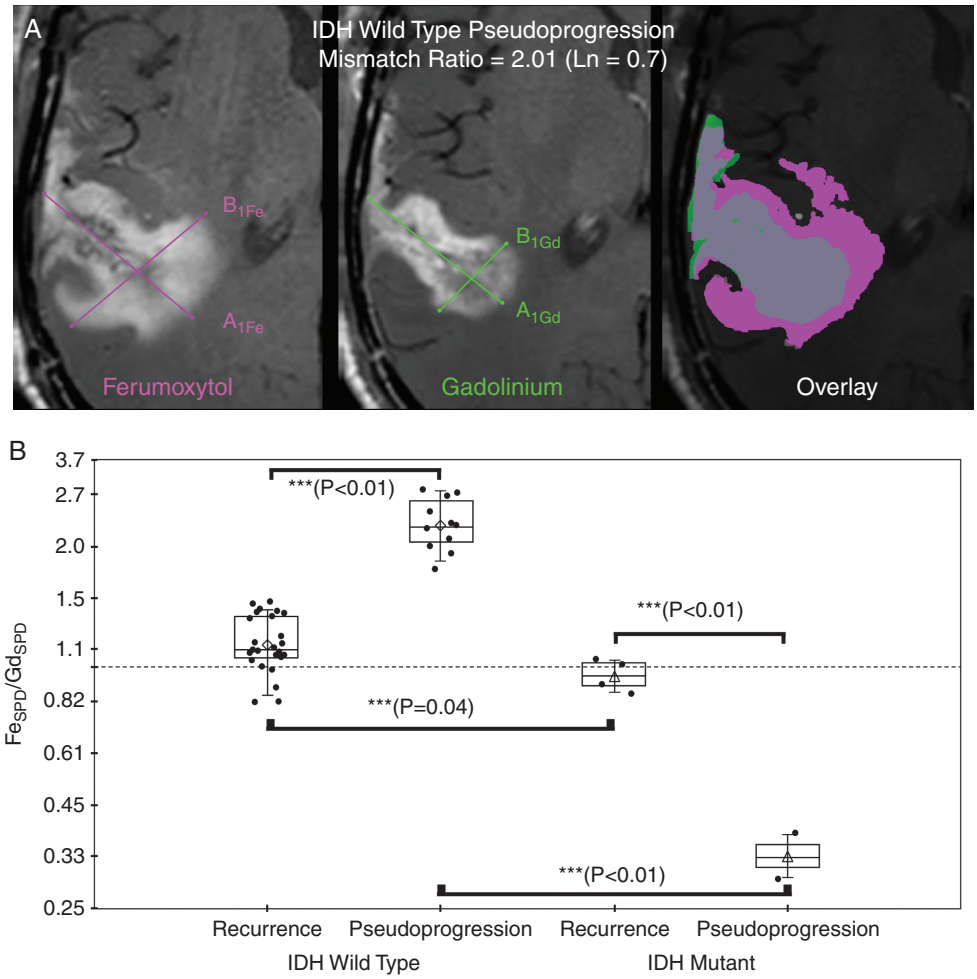

Fig. 2 Representative example of ferumoxytol (Fe, left) and gadolinium (Gd, middle) SPD measurement (A) and graph of mean natural log ratio measurements (B) categorized by final disease status and IDH-1 mutational status. (A) Sum of products diameter (SPD) was calculated for 24-hour delayed ferumoxytol enhanced phase (left image) and gadolinium enhanced (middle image) T1-weighted images; SPD = A1 × B1 at maximal site of enhancement according to RANO guidelines. Contrast enhancement mismatch was calculated as the natural log ratio of SPDFe/SPDGd. For statistical analysis, the natural log of the enhancement mismatch ratio was used so that nonlinearities in ratio variables could be linearized such that the ratios are equidistant and the dependent variable is not weighted in favor of the denominator. For illustrative purposes; fused imaged overlay (ferumoxytol enhancing region, pink; gadolinium enhancing region, green; enhancing overlap, gray; right image) demonstrates the degree of ferumoxytol/gadolinium mismatch in an IDH-1 wild type patient with pseudoprogression. (B) Box plot of cohort enhancement mismatch values as the ratio categorized by final disease status (disease recurrence or pseudoprogression) and IDH-1 mutational status demonstrates contrast enhancement mismatch ratio was found to be significantly different at all posttherapy timepoints when assessed by ANOVA (***denotes statistical significance). Significantly elevated enhancement mismatch ratios were observed in patients with recurrent IDH-1 wild type glioblastoma compared with patients with recurrent IDH-1 mutated glioblastoma (0.13 ± 0.17 vs –0.05 ± 0.09, $P = 0.04$). Additionally, IDH-1 wild type pseudoprogression was significantly elevated compared with IDH-1 wild type recurrent disease (0.82 ± 0.15 vs 0.13 ± 0.17, $P < 0.01$).

ferumoxytol enhancement SPD to gadolinium SPD. The natural log was used so that nonlinearities in ratio variables could be linearized such that the ratios are equidistant and the dependent variable is not weighted in favor of the denominator. For example, the ratios of 5/2 and 2/5 are not equidistant from one until the natural log is performed [Ln(5/2) = 0.92 and Ln(2/5) = –0.92]. This allows for centering of the displacement of the relationship evenly around zero irrespective of which variable is in the numerator or denominator. When stratified by molecular profiles and clinical status, dual contrast enhancement mismatch ratio allowed for assessment of differences by 2-way ANOVA using pairwise multiple comparison and Student's *t*-test (SigmaStat for Windows 3.5, Systat Software). Intraclass correlation coefficients were calculated to assess reviewer agreement. Receiver operator curve analysis provided an optimal cutoff value allowing for the determination of diagnostic performance. Overall patient survival

was calculated from the initiation of treatment until death. Survival analysis was performed using a log-rank test. *P*-value <0.05 was considered to indicate a statistically significant difference in all tests.

Results

Comparison of Contrast Enhancement Mismatch by IDH-1 Mutation and Disease Status

Within the IDH-1 wild type cohort, the contrast enhancement mismatch was significantly elevated at time of pseudoprogression [mean ± SD (0.82 ± 0.15) (natural log ratio; please note that Ln(1) = 0, Ln(2) = 0.69, and Ln(3) = 1.10)]; relative to disease recurrence (0.13 ± 0.17; $P < 0.01$; Fig. 2B). Enhancement mismatch was significantly reduced in pseudoprogression patients with IDH mutation (–1.06 ± 0.19) compared with patients with IDH mutated disease recurrence (–0.05 ± 0.10; $P < 0.01$; Supplementary Figure 1). Contrast enhancement mismatch was significantly elevated in patients with IDH-1 wild type glioblastoma at all posttherapy timepoints compared with patients with IDH-1 mutation (Table 1; $P < 0.05$). A 2-way ANOVA on contrast enhancement mismatch was performed with IDH-1 and disease status as independent variables. The main effects of IDH-1 status and disease status were both significant ([F(degree of freedom)]: F(1,38) = 197.3 and 5.6, $P < 0.001$ and .03, respectively. Importantly, the interaction effect of IDH-1 status × disease status was statistically significant, F(1,38) = 135.7, $P < 0.001$. There was no significant difference in gadolinium or ferumoxytol SPD when categorized by IDH-1 status, disease status, imaging timepoint, or as a cohort.

Comparison of Contrast Enhancement Mismatch by Clinically Relevant MRI Timepoints and Disease Status

Contrast enhancement mismatch increased significantly at the time of pseudoprogression (0.81 ± 0.15) relative to prior imaging timepoints in IDH-1 wild type patients (0.01 ± 0.17; $P < 0.01$; Fig. 3A). In IDH-1 mutated patients, there was a trend toward decreased mismatch values in patients who developed pseudoprogression compared with prior imaging timepoints. However, this difference did not reach statistical significance ($P = 0.051$). A difference from baseline was not observed to be statistically significant in patients with disease recurrence.

Comparison of Contrast Enhancement Mismatch by MGMT Promoter Methylation and Disease Status

Twenty-three patients were found to have MGMT promoter methylation and 22 patients were found to have a nonmethylated MGMT promoter. Patients with nonmethylated MGMT promoter who developed pseudoprogression ($N = 9$, mismatch = 0.64 ± 0.6) demonstrated significantly increased contrast enhancement mismatch compared with patients with nonmethylated MGMT recurrent disease ($N = 16$, 0.14 ± 0.14; $P = 0.04$). No significant difference between contrast enhancement mismatch was observed in patients with methylated MGMT promoter. Additionally, there were no significant differences in contrast enhancement mismatch or SPD between methylated and nonmethylated MGMT promoter groups at any of the other imaging timepoints.

Diagnostic Utility of Contrast Enhancement Mismatch and Clinical Outcomes

Receiver operating characteristic curve analysis identified contrast enhancement mismatch threshold values of 0.56 for IDH-1 wild type and –0.89 for IDH-1 mutated patients as optimal cutoff values for the diagnosis of pseudoprogression (100% sensitivity and specificity in this cohort). The positive and negative predictive values for the diagnosis of pseudoprogression were 100% using the threshold values. Survival analysis for the entire cohort demonstrated

Table 1 Analysis of contrast mismatch by IDH-1 mutational status and imaging timepoint

	Preoperative	Postoperative	Postradiation	Follow-up	Disease Recurrence	Pseudoprogression	Resolving Pseudoprogression
IDH-1 wild type	0.02 (0.15)	0.10 (0.10)	0.21 (0.17)	0.08 (0.17)	0.13 (0.17)	0.82 (0.15)	–0.10 (0.14)
IDH-1 mutated	0.03 (0.32)	None	–0.12 (0.02)	–0.07 (0.07)	–0.05 (0.09)	–1.10 (0.19)	None
P-value	0.98	NA	<0.01	0.04	0.02	0.05	NA

Note: Reported values are the natural log ratio of SPD, ferumoxytol to gadolinium mismatch. Note that Ln(1) = 0, Ln(2) = 0.69, and Ln(3) = 1.10. Positive value reflects increased ratio from zero. Negative value reflects decreased ratio from zero. Wild type = no mutation detected; mutated = mutation detected; preoperative = MRI examination occurred prior to surgical resection; postoperative = MRI examination occurred after maximally safe surgical resection but prior to radiation therapy; postradiation = MRI examination occurred within 3 months following last date of radiation therapy; follow-up = MRI examination occurred more than 3 months following last date of radiation therapy but before disease status was diagnosed; disease recurrence = progression of disease defined by RANO criteria or histological sampling; pseudoprogression = lesion with subsequent resolution of enhancing focus; resolving pseudoprogression = MRI examination occurred following diagnosis of pseudoprogression. Example: Difference between e^x SPD ferumoxytol/gadolinium mismatch of 0.82 and –1.1 would be 1.92, which is an absolute difference of 682%.

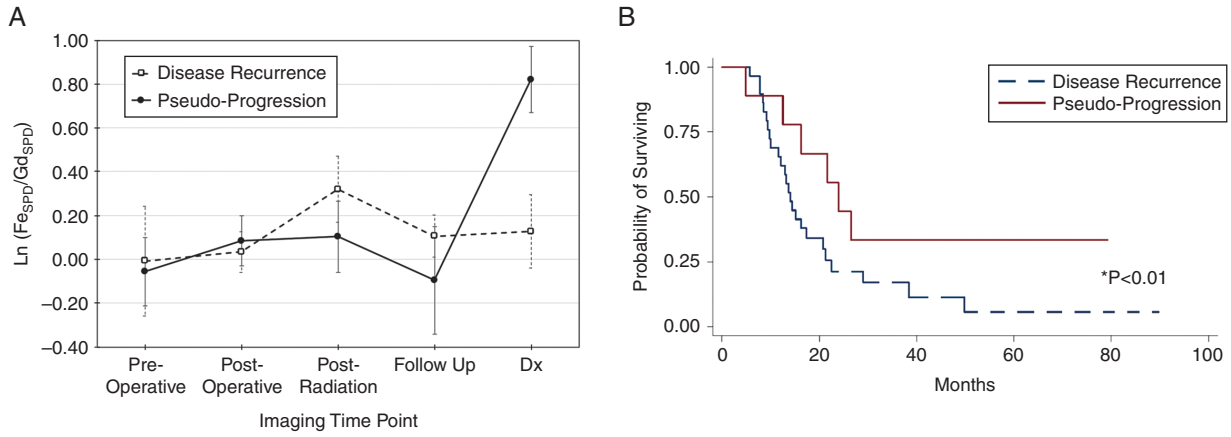

Fig. 3 Graphs of contrast mismatch ratio by clinically relevant timepoints (A) and Kaplan–Meier survival curve of the entire patient cohort categorized by disease recurrence or pseudoprogression (B). (A) Graph of natural log contrast enhancement mismatch ratio as a function of imaging timepoints in patients with IDH-1 wild type glioblastoma. The mean enhancing mismatch ratio increases significantly at the time of pseudoprogression (solid line) compared with prior imaging timepoints ($P < 0.01$). Conversely, mean enhancing mismatch ratio in patients with disease recurrence (dashed line) does not significantly change compared with prior imaging timepoints. (B) Kaplan–Meier survival curve of the patient cohort demonstrates significantly prolonged survival for patients with pseudoprogression (red line) compared with disease recurrence (blue dashed line).

that patients with pseudoprogression demonstrated significantly prolonged overall survival (20.0 ± 10.2 mo) compared with those with recurrent disease (15.9 ± 10.1 mo; Z = 2.01, $P = 0.04$) (Fig. 3B).

Histopathological Observations

Standard of care stereotactic tissue sampling was performed in 3 patients with IDH-1 wild type glioblastoma (1 patient with newly diagnosed disease and 2 patients with recurrent disease) to facilitate diagnosis. Tissue sampling sites were categorized by the presence of ferumoxytol or gadolinium enhancement on T1-weighted imaging. Sites with only ferumoxytol enhancement were characterized by activated microglia and low cellularity infiltrative tumor (newly diagnosed disease) or CRT-induced changes evidenced by widespread vascular hyalinization with scattered macrophages in the absence of viable tumor (disease recurrence) (Fig. 4). Dual contrast enhancing sites demonstrated highly cellular tumor with microvascular proliferation and epithelioid TAM which appeared similar between patients with newly diagnosed and recurrent disease. Tissue specimens obtained from central non-enhancing regions demonstrated tissue necrosis without evidence of viable tumor.

Interrater Reliability and Impact of Bevacizumab and Dexamethasone on Enhancement Mismatch

Interrater reliability of SPD measurements was high ($ICC_{ferumoxytol}$ = 0.99, $ICC_{gadolinium}$ = 0.99). Twenty-four patients received dexamethasone concurrently with Fe-MRI (mean ± SD, 3.66 ± 4.73 mg). Eleven of the patients (10 IDH wild type) received dexamethasone at the time of disease recurrence (6.5 ± 4.14 mg). One IDH wild type patient received dexamethasone at the time of pseudoprogression (12 mg). There was a trend toward reduced mismatch values for IDH wild type patients with disease recurrence who received dexamethasone (0.06 ± –1.66) compared with those who did not receive dexamethasone (0.19 ± –1.77); however, this did not reach statistical significance ($P = 0.06$). The one patient with IDH wild type pseudoprogression who received dexamethasone had a mismatch value of 0.83, which was within the range of mismatch values for IDH wild type pseudoprogression (0.82 ± 0.15; minimum cohort value, 0.56; maximum cohort value, 1.02). A total of 5 patients (all IDH wild type) received bevacizumab (10 mg/kg) within 1 month of Fe-MRI. Three of the patients (2 with tumor recurrence and 1 pseudoprogression) received bevacizumab the same day as ferumoxytol administration. Two of the patients with tumor recurrence received bevacizumab within 1 month prior to ferumoxytol administration (25.5 ± 6.4 days). No significant difference in enhancement mismatch was observed between patients with recurrent disease who received bevacizumab (0.004 ± 0.14) and those who did not (0.15 ± 0.16; $P = 0.13$). The one patient with pseudoprogression who received ferumoxytol and bevacizumab concurrently demonstrated a mismatch value of 0.65, which was within the range of mismatch values for IDH wild type pseudoprogression (0.82 ± 0.15; minimum cohort value, 0.56; maximum cohort value, 1.02).

Discussion

In this retrospective study, we investigated whether the use of ferumoxytol and gadolinium contrast enhancement mismatch ratios on T1-weighted MRI could identify

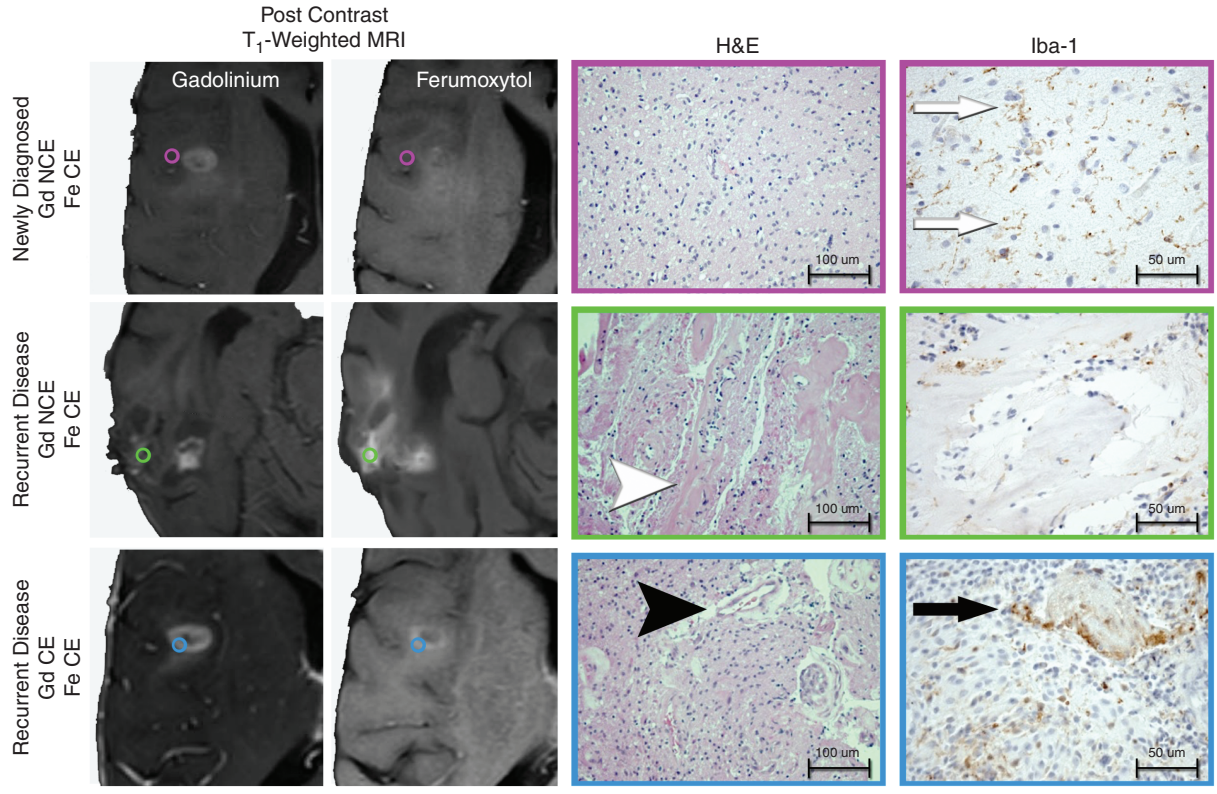

Fig. 4 Histopathological observation of regional image guided tissue samples based on ferumoxytol and gadolinium contrast enhancing patterns. Standard of care stereotactic tissue sampling was performed in 3 patients with IDH-1 wild type glioblastoma at the time of initial diagnosis or at the time of disease recurrence. Tissue samples were classified by the presence of gadolinium (Gd, left column) or ferumoxytol (Fe, middle left column) contrast enhancement (CE). Tissue specimens were histopathologically characterized for the presence of tumor and microvascular proliferation (hematoxylin and eosin; middle right column; 100 μm scale bar) and the presence of activated microglia/macrophage (ionized calcium binding adaptor molecule 1 [Iba-1; 50 μm scale bar]). Regions of ferumoxytol contrast enhancement and gadolinium noncontrast enhancement (NCE) were observed in patients with newly diagnosed glioblastoma (top) and disease recurrence (middle). Ferumoxytol-only enhancing regions in patients with newly diagnosed IDH-1 wild type glioblastoma demonstrated infiltrating glioma with low cellularity, delicate vasculature, and activated microglia (white arrows; brown staining Iba-1 cells). Ferumoxytol-only enhancing regions in patients with recurrent IDH-1 wild type glioblastoma demonstrated therapeutic changes evidenced by widespread vascular hyalinization (white arrow head) with scattered macrophages without evidence of viable tumor. Dual contrast enhancing sites (bottom row) appeared biologically similar in the newly diagnosed and disease recurrence setting being characterized by highly cellular tumor with microvascular proliferation (black arrow head) and TAMs with an epithelioid appearance (black arrow).

the development of neuroinflammation-mediated pseudoprogression in patients with glioblastoma. Our results suggest that the SPD ratio of ferumoxytol to gadolinium enhancement, and not simply the SPD measurement of either contrast agent alone, is a sensitive and specific biomarker capable of distinguishing pseudoprogression from disease recurrence in patients with glioblastoma. Taken together, these findings suggest that combined Fe- and Gd-MRI characterizes glioblastoma CRT-induced neuroinflammation. If prospectively validated, this imaging paradigm has the immediate potential to impact treatment response assessment, timing of therapy, and method of disease monitoring. Furthermore, this noninvasive imaging methodology could potentially affect the clinical outcome of patients with glioblastoma by improving endpoint specificity in clinical trials by correctly differentiating pseudoprogression from disease recurrence.

Our study suggests the diagnostic utility of ferumoxytol to gadolinium contrast enhancement mismatch ratio in the evaluation of glioblastoma response to CRT. Surgical tissue sampling or watchful waiting for the reduction of enhancement on follow-up Gd-MRI is the current standard of care.[38–41]Tissue sampling is fraught with sampling errors and inconsistent diagnostic criteria.[39] Great strides have been made to overcome the limitations of T1-weighted Gd-MRI by developing perfusion Gd-MRI (CBV) and amino acid PET techniques as quantifiable diagnostic measures of pseudoprogression. The scientific premise for the use of these imaging characteristics is that microvascular proliferation (CBV) and tissue protein synthesis rates (amino acid PET) are better quantifiable metrics of pseudoprogression than the subjective assessment of vascular leakiness (Gd-T1 weighted enhancement). A meta-analysis of 416 patients by Wan et al demonstrated a pooled sensitivity of

0.88 and specificity of 0.77 for Gd-MRI CBV to differentiate recurrent glioblastoma from pseudoprogression.[42] Galldiks et al have explored the use of dynamic and static O-(2-[18F]fluoroethyl)-L-tyrosine (FET) PET imaging in 124 patients with glioma (33 glioblastoma at time of first recurrence) with concern for disease progression according to RANO criteria. Individual metric analysis yielded moderate sensitivity (68% to 82%) and high specificity (73% to 100%). A combined dynamic and static metric analysis showed improved diagnostic capabilities (sensitivity of 93% and specificity of 100%).[43] Dynamic susceptibility contrast (DSC) perfusion and amino acid PET imaging techniques do provide improved diagnostic capabilities compared with T1-weighted Gd-enhanced MRI.[32] However, there are significant technical and biological limitations. From a technical perspective, amino acid PET and Gd-DSC perfusion can be challenging to clinically implement due to postprocessing demands (time-consuming dynamic PET metric analysis and need for leakage correction for DSC CBV calculation). Furthermore, susceptibility artifacts that arise from tumor location (air–bone interface) or intrinsic blood products often limit the clinical utility. Finally, biologically mediated limitations include the overlap in metabolic characteristics within both pseudoprogression and tumor regrowth when assessed by Gd-CBV and amino acid PET. The persistent diagnostic inaccuracy of these advanced imaging techniques is likely a result of not specifically characterizing the biological process by which pseudoprogression develops: innate immune mediated neuroinflammation. Our results suggest that the use of ferumoxytol with gadolinium contrast enhancement mismatch ratio may improve upon current imaging techniques as a biomarker of therapy mediated neuroinflammation, thereby providing additional diagnostic information that is useful in differentiating glioblastoma recurrence from pseudoprogression.

The preliminary histological observations of our study suggest that activation of innate immunity may play a role in the degree of observed contrast enhancement mismatch. This finding is consistent with prior preclinical observations by McConnell et al.[34] Tissue samples obtained from regions of only ferumoxytol enhancement demonstrated activated microglia and/or TAMs in a background of treatment-related vascular hyalinization without evidence of viable tumor. The current pathophysiological understanding of pseudoprogression is that the phenomenon is CRT induced and neuroinflammatory in etiology with recruitment of TAMs to the tumor and surrounding tissue.[44–48] Thus, an imaging biomarker of TAM accumulation, such as ferumoxytol, may be better suited to localizing pseudoprogression than gadolinium contrast alone. As such, the mismatch ratio of ferumoxytol and gadolinium enhancement observed in our study is hypothesized to be a marker of innate immune activation.

Our results suggest that the innate immunological response mechanism to CRT may vary by IDH-1 mutational status.[47] The observed differences in enhancement mismatch may suggest that the immunological response mechanisms vary by IDH-1 mutational status. As a Krebs cycle enzyme, IDH-1 functions in the oxidative carboxylation of isocitrate to create α-ketoglutarate via reduction of NADPH.[18] The production of NADPH is necessary for the regeneration of reduced glutathione, a key cellular antioxidant essential for the phagocytic activity of antigen presenting cells such as macrophages, among other immune system functions.[49,50] In IDH-1 mutants, a reduction in glutathione content may result in less TAM phagocytosis and ferumoxytol uptake. Additionally, as α-ketoglutarate levels decrease, hypoxia-inducible factor 1 is less effectively degraded, resulting in a decrease in hypoxia-related TAM infiltration. As such, decreased levels of TAMs that demonstrate functionally reduced ability for phagocytosis within IDH-1 mutant glioblastoma undergoing pseudoprogression may account for the markedly decreased mismatch ratios that we observed, although this is entirely speculative.

This study has several important limitations. First, our small sample size and the retrospective nature of our study caution against overinterpretation of our findings. Moreover, the mutant IDH-1 group contained only 6 patients. While this number exceeds the proportion of mutant IDH-1 expected in a cohort of this size, it is difficult to infer clinically significant interpretations from such a small sample size. However, due to the limitation of mutant IDH-1 incidence in glioblastoma, we believe that this report is an important first step that will lay the foundation for larger studies. Future prospective investigations should attempt to verify these imaging characteristics within a separate, larger cohort of patients. Second, we recognize that our study is limited by the absence of correlative biological analysis to determine the mechanism for the observed enhancement mismatch differences between patients with IDH-1 wild type and mutated tumors. Nor have we provided definitive histopathologic confirmation of TAM associated neuroinflammation within sites of enhancement mismatch. While TAM mediated neuroinflammation is one proposed mechanism for the observed enhancement mismatch, future validation should include image guided tissue sampling to verify the biological processes accounting for this imaging finding. Finally, our small sample size precluded subgroup survival analysis to determine whether the observed MR imaging characteristics were associated with improved clinical outcomes.

Conclusion

Our study provides early retrospective evidence that glioblastoma pseudoprogression can be diagnosed by the use of both ferumoxytol and gadolinium contrast enhanced MRI. Specifically, patients with IDH-1 wild type nonmethylated MGMT glioblastoma treated with standard of care temozolomide-based CRT develop regions of pseudoprogression specifically characterized by markedly increased ferumoxytol to gadolinium contrast enhancement mismatch.

Supplementary Material

Supplementary data are available at *Neuro-Oncology* online.

Keywords

ferumoxytol | glioblastoma | macrophage | pseudoprogression | RANO

Funding

This work was supported in part by National Institutes of Health grants CA199111 (E.A.N), CA137488-15S1 (R.F.B and E.A.N) and L30 CA220897-01 (R.F.B) by the Walter S. and Lucienne Driskill Foundation (E.A.N), and by a Veterans Administration Merit Review grant (E.A.N).

Acknowledgments

The first author thanks Bethany Barajas MSN for her helpful comments regarding this paper, Ann Mitchell for her helpfulness in the operating room, and the many wonderful patients included in this study who selflessly contributed their time to undergo research medical imaging while dealing with a deadly disease.

Conflict of interest statement. No conflicts.

Authorship statement. RFB and BEH performed all aspects of study design, acquisition, analysis, and interpretation of data, drafted the manuscript, and approved the final version. DS, HLM, and DRP substantially contributed to concept and design of work, analysis, and interpretation of data, drafted manuscript, and approved final version. AH, LS, CGV, and JF substantially contributed to analysis and interpretation of data, drafted manuscript, and approved final version. JJJ, CDK, AMR, AD, JSC, JC, SJH, PA, LLM, RW, and WDR substantially contributed to analysis and interpretation of data, revised manuscript, and approved final version. EAN substantially contributed to the conception or design of the work, acquisition, and interpretation of data, revised manuscript, and approved final version.

References

1. Hottinger AF, Stupp R, Homicsko K. Standards of care and novel approaches in the management of glioblastoma multiforme. *Chin J Cancer.* 2014;33(1):32–39.
2. Stupp R, Mason WP, van den Bent MJ, et al; European Organisation for Research and Treatment of Cancer Brain Tumor and Radiotherapy Groups; National Cancer Institute of Canada Clinical Trials Group. Radiotherapy plus concomitant and adjuvant temozolomide for glioblastoma. *N Engl J Med.* 2005;352(10):987–996.
3. Stupp R, Hegi ME, Mason WP, et al; European Organisation for Research and Treatment of Cancer Brain Tumour and Radiation Oncology Groups; National Cancer Institute of Canada Clinical Trials Group. Effects of radiotherapy with concomitant and adjuvant temozolomide versus radiotherapy alone on survival in glioblastoma in a randomised phase III study: 5-year analysis of the EORTC-NCIC trial. *Lancet Oncol.* 2009;10(5):459–466.
4. Mirimanoff R, Stupp R. Long-term survival in glioblastoma possible. Updated results of the EORTC/NCIC phase III randomized trial on radiotherapy (RT) and concomitant and adjuvant temozolomide (TMZ) versus RT alone. *Int J Radiat Oncol Biol Phys.* 2007;69:S2.
5. Hegi ME, Diserens AC, Gorlia T, et al. MGMT gene silencing and benefit from temozolomide in glioblastoma. *N Engl J Med.* 2005;352(10):997–1003.
6. Keime-Guibert F, Chinot O, Taillandier L, et al; Association of French-Speaking Neuro-Oncologists. Radiotherapy for glioblastoma in the elderly. *N Engl J Med.* 2007;356(15):1527–1535.
7. Malmström A, Grønberg BH, Marosi C, et al; Nordic Clinical Brain Tumour Study Group (NCBTSG). Temozolomide versus standard 6-week radiotherapy versus hypofractionated radiotherapy in patients older than 60 years with glioblastoma: the Nordic randomised, phase 3 trial. *Lancet Oncol.* 2012;13(9):916–926.
8. Taal W, Brandsma D, de Bruin HG, et al. Incidence of early pseudo-progression in a cohort of malignant glioma patients treated with chemoir-radiation with temozolomide. *Cancer.* 2008;113(2):405–410.
9. Brandes AA, Franceschi E, Tosoni A, et al. MGMT promoter methylation status can predict the incidence and outcome of pseudoprogression after concomitant radiochemotherapy in newly diagnosed glioblastoma patients. *J Clin Oncol.* 2008;26(13):2192–2197.
10. Fabi A, Russillo M, Metro G, Vidiri A, Di Giovanni S, Cognetti F. Pseudoprogression and MGMT status in glioblastoma patients: implications in clinical practice. *Anticancer Res.* 2009;29(7):2607–2610.
11. Gerstner ER, McNamara MB, Norden AD, Lafrankie D, Wen PY. Effect of adding temozolomide to radiation therapy on the incidence of pseudoprogression. *J Neurooncol.* 2009;94(1):97–101.
12. Wen PY, Kesari S. Malignant gliomas in adults. *N Engl J Med.* 2008;359(5):492–507.
13. Wen PY, Macdonald DR, Reardon DA, et al. Updated response assessment criteria for high-grade gliomas: Response Assessment in Neuro-Oncology Working Group. *J Clin Oncol.* 2010;28(11):1963–1972.
14. Gahramanov S, Muldoon LL, Varallyay CG, et al. Pseudoprogression of glioblastoma after chemo- and radiation therapy: diagnosis by using dynamic susceptibility-weighted contrast-enhanced perfusion MR imaging with ferumoxytol versus gadoteridol and correlation with survival. *Radiology.* 2013;266(3):842–852.
15. Weller M, Pfister SM, Wick W, Hegi ME, Reifenberger G, Stupp R. Molecular neuro-oncology in clinical practice: a new horizon. *Lancet Oncol.* 2013;14(9):e370–e379.
16. Li H, Li J, Cheng G, Zhang J, Li X. IDH mutation and MGMT promoter methylation are associated with the pseudoprogression and improved prognosis of glioblastoma multiforme patients who have undergone concurrent and adjuvant temozolomide-based chemoradiotherapy. *Clin Neurol Neurosurg.* 2016;151:31–36.
17. Weller M, Felsberg J, Hartmann C, et al. Molecular predictors of progression-free and overall survival in patients with newly diagnosed glioblastoma: a prospective translational study of the German Glioma Network. *J Clin Oncol.* 2009;27(34):5743–5750.
18. Ushio-Fukai M, Nakamura Y. Reactive oxygen species and angiogenesis: NADPH oxidase as target for cancer therapy. *Cancer Lett.* 2008;266(1):37–52.
19. Wang J, Yi J. Cancer cell killing via ROS: to increase or decrease, that is the question. *Cancer Biol Ther.* 2008;7(12):1875–1884.
20. Kim JM, Kim H, Kwon SB, et al. Intracellular glutathione status regulates mouse bone marrow monocyte-derived macrophage differentiation and phagocytic activity. *Biochem Biophys Res Commun.* 2004;325(1):101–108.

21. Ghezzi P. Role of glutathione in immunity and inflammation in the lung. *Int J Gen Med.* 2011;4:105–113.
22. Cohen AL, Holmen SL, Colman H. IDH1 and IDH2 mutations in gliomas. *Curr Neurol Neurosci Rep.* 2013;13(5):345.
23. Garber K. Oncometabolite? IDH1 discoveries raise possibility of new metabolism targets in brain cancers and leukemia. *J Natl Cancer Inst.* 2010;102(13):926–928.
24. Murdoch C, Giannoudis A, Lewis CE. Mechanisms regulating the recruitment of macrophages into hypoxic areas of tumors and other ischemic tissues. *Blood.* 2004;104(8):2224–2234.
25. Lewis JS, Lee JA, Underwood JC, Harris AL, Lewis CE. Macrophage responses to hypoxia: relevance to disease mechanisms. *J Leukoc Biol.* 1999;66(6):889–900.
26. Wang SC, Hong JH, Hsueh C, Chiang CS. Tumor-secreted SDF-1 promotes glioma invasiveness and TAM tropism toward hypoxia in a murine astrocytoma model. *Lab Invest.* 2012;92(1):151–162.
27. Palazon A, Goldrath AW, Nizet V, Johnson RS. HIF transcription factors, inflammation, and immunity. *Immunity.* 2014;41(4):518–528.
28. Ellingson BM, Chung C, Pope WB, Boxerman JL, Kaufmann TJ. Pseudoprogression, radionecrosis, inflammation or true tumor progression? Challenges associated with glioblastoma response assessment in an evolving therapeutic landscape. *J Neurooncol.* 2017;134(3):495–504.
29. Young RJ, Gupta A, Shah AD, et al. Potential utility of conventional MRI signs in diagnosing pseudoprogression in glioblastoma. *Neurology.* 2011;76(22):1918–1924.
30. Shah AH, Snelling B, Bregy A, et al. Discriminating radiation necrosis from tumor progression in gliomas: a systematic review what is the best imaging modality? *J Neurooncol.* 2013;112(2):141–152.
31. Mullins ME, Barest GD, Schaefer PW, Hochberg FH, Gonzalez RG, Lev MH. Radiation necrosis versus glioma recurrence: conventional MR imaging clues to diagnosis. *AJNR Am J Neuroradiol.* 2005;26(8):1967–1972.
32. Verma N, Cowperthwaite MC, Burnett MG, Markey MK. Differentiating tumor recurrence from treatment necrosis: a review of neuro-oncologic imaging strategies. *Neuro Oncol.* 2013;15(5):515–534.
33. Albert NL, Weller M, Suchorska B, et al. Response Assessment in Neuro-Oncology working group and European Association for Neuro-Oncology recommendations for the clinical use of PET imaging in gliomas. *Neuro Oncol.* 2016;18(9):1199–1208.
34. McConnell HL, Schwartz DL, Richardson BE, Woltjer RL, Muldoon LL, Neuwelt EA. Ferumoxytol nanoparticle uptake in brain during acute neuroinflammation is cell-specific. *Nanomedicine.* 2016;12(6):1535–1542.
35. Toth GB, Varallyay CG, Horvath A, et al. Current and potential imaging applications of ferumoxytol for magnetic resonance imaging. *Kidney Int.* 2017;92(1):47–66.
36. Weissleder R, Nahrendorf M, Pittet MJ. Imaging macrophages with nanoparticles. *Nat Mater.* 2014;13(2):125–138.
37. Neuwelt A, Sidhu N, Hu CA, Mlady G, Eberhardt SC, Sillerud LO. Iron-based superparamagnetic nanoparticle contrast agents for MRI of infection and inflammation. *AJR Am J Roentgenol.* 2015;204(3):W302–W313.
38. Khan MN, Sharma AM, Pitz M, et al. High-grade glioma management and response assessment—recent advances and current challenges. *Curr Oncol.* 2016;23(4):e383–e391.
39. Melguizo-Gavilanes I, Bruner JM, Guha-Thakurta N, Hess KR, Puduvalli VK. Characterization of pseudoprogression in patients with glioblastoma: is histology the gold standard? *J Neurooncol.* 2015;123(1):141–150.
40. Brandsma D, Stalpers L, Taal W, Sminia P, van den Bent MJ. Clinical features, mechanisms, and management of pseudoprogression in malignant gliomas. *Lancet Oncol.* 2008;9(5):453–461.
41. Knudsen-Baas KM, Moen G, Fluge O, Storstein A. Pseudo-progression in high-grade glioma. *Acta Neurol Scand Suppl.* 2013:31–37.
42. Wan B, Wang S, Tu M, Wu B, Han P, Xu H. The diagnostic performance of perfusion MRI for differentiating glioma recurrence from pseudoprogression: a meta-analysis. *Medicine (Baltimore).* 2017;96(11):e6333. https://www.ncbi.nlm.nih.gov/pubmed/28296759
43. Galldiks N, Dunkl V, Stoffels G, et al. Diagnosis of pseudoprogression in patients with glioblastoma using O-(2-[18F]fluoroethyl)-L-tyrosine PET. *Eur J Nucl Med Mol Imaging.* 2015;42(5):685–695.
44. Taal W, Brandsma D, de Bruin HG, et al. Incidence of early pseudo-progression in a cohort of malignant glioma patients treated with chemoirradiation with temozolomide. *Cancer.* 2008;113(2):405–410.
45. de Wit MC, de Bruin HG, Eijkenboom W, Sillevis Smitt PA, van den Bent MJ. Immediate post-radiotherapy changes in malignant glioma can mimic tumor progression. *Neurology.* 2004;63(3):535–537.
46. Van Mieghem E, Wozniak A, Geussens Y, et al. Defining pseudoprogression in glioblastoma multiforme. *Eur J Neurol.* 2013;20(10):1335–1341.
47. Wang SC, Yu CF, Hong JH, Tsai CS, Chiang CS. Radiation therapy-induced tumor invasiveness is associated with SDF-1-regulated macrophage mobilization and vasculogenesis. *PLoS One.* 2013;8(8):e69182.
48. Vatner RE, Formenti SC. Myeloid-derived cells in tumors: effects of radiation. *Semin Radiat Oncol.* 2015;25(1):18–27.
49. Brandsma D, Stalpers L, Taal W, Sminia P, van den Bent MJ. Clinical features, mechanisms, and management of pseudoprogression in malignant gliomas. *Lancet Oncol.* 2008;9(5):453–461.
50. Vatner RE, Formenti SC. Myeloid-derived cells in tumors: effects of radiation. *Semin Radiat Oncol.* 2015;25(1):18–27.